

# Evaluation of the Frequency-Dependent Young's Modulus and Damping Factor of Rubber from Experiment and Their Implementation in a Finite-Element Analysis

D. Koblar<sup>1</sup> and M. Boltežar<sup>2</sup>

<sup>1</sup> Domel d.o.o., Železniki, Slovenia

<sup>2</sup> Faculty of Mechanical Engineering, University of Ljubljana, Ljubljana, Slovenia

## Keywords

Dynamic Material Properties of Rubber, Young's Modulus, Damping Factor

## Correspondence

M. Boltežar,  
Faculty of Mechanical Engineering,  
University of Ljubljana,  
Aškerčeva 6,  
1000 Ljubljana,  
Slovenia.  
Email: miha.boltezar@fs.uni-lj.si

Received: November 21, 2012;  
accepted: August 30, 2013

doi:10.1007/s40799-016-0027-7

## Abstract

Rubbers are commonly used in industry to reduce vibration transfer and, consequently, reduce structural noise. The vibration transfer through rubber can be modelled with finite elements; however, to achieve satisfactory results it is necessary to know the viscoelastic properties of the rubber. This paper describes the commonly used theory of vibration transmission through rubber modelled as a single-degree-of-freedom (SDOF) system. Three simplified rubber models are used to identify the constant Young's modulus and damping factor from the measurements of two different rubber specimens, and with the obtained results the theoretical transmissibilities are calculated. The frequency-dependent Young's modulus and damping factor are also calculated from measurements. The practical use of previous measurements of dynamic material properties is presented in a finite-element analysis, where three different definitions of the dynamic material properties are carried out for four different rubber specimens, which corresponds to 12 analyses. The finite-element analyses are then compared with the measurements, and general guidelines for using dynamic material properties in ANSYS Workbench v.14 are given.

## Introduction

Rubber materials are commonly used to control structural vibrations and sound radiation. However, to predict the vibration response of a system the dynamic characteristics of rubber, such as the Young's modulus and the damping factor, must be accurately identified.

Because of the viscoelastic behaviour of the rubber material, its dynamic material properties, which depend on many environmental and operating conditions, but mainly on the static preload, vibration amplitude, temperature and frequency,<sup>1</sup> are difficult to define. From the theory of viscoelasticity,<sup>2</sup> it is known that at least two parameters are needed to completely define the mechanical behaviour of an isotropic viscoelastic material. Usually these two parameters are the Young's and bulk moduli or one modulus and the Poisson's ratio of the viscoelastic material.

In the literature, many authors have conducted experimental research by directly measuring the Young's modulus and the damping factor. Sim and Kim,<sup>3</sup> for example, developed a technique to estimate the material properties of viscoelastic materials for use with finite-element method (FEM) applications. They derived the Young's modulus, the damping factor, and the Poisson's ratio from two different rubbers with various shape factors (one with a small factor and one with a large). A similar test method for characterizing the dynamic behaviour of rubber compounds was presented by Ramorino et al.<sup>4</sup> and their results were also compared using the dynamic mechanical thermal analyzer (DMTA), which showed good agreement. Additionally, Caracciolo et al.<sup>5,6</sup> presented measurements of the complex Poisson's ratio and Young's modulus versus frequency, which were performed on simple, beam-like specimens. One of the drawbacks of the mentioned test methods is

the inability to statically preload the test specimen to whatever preload may be desired, because the only way to preload the test specimen is to add mass, which results in large loads on the shaker.

The dynamic stiffness was also studied instead of the dynamic modulus through the receptance of the specimen, where the impact hammer replaced the shaker as the source of the vibration. Lin et al.<sup>7</sup> developed a method to evaluate the frequency-dependent rubber mount's stiffness and damping characteristics by utilizing the measured complex frequency response function from the impact test. Ooi and Ripin<sup>8</sup> simultaneously measured the dynamic driving-point stiffness and the dynamic transfer stiffness and made a comparison with the previously mentioned method developed by Lin et al.<sup>7</sup> The authors showed that in the low-frequency range the dynamic driving-point stiffness can be used to represent the dynamic transfer stiffness, but with an increase of the frequency the inertial force gets bigger compared to the elastic force in the system; therefore, the dynamic stiffness starts to deviate significantly. Nadeau and Champoux<sup>9</sup> made a comparison of engine mount complex stiffness in axial and lateral direction using blocked transfer stiffness and Hao et al.<sup>10</sup> used dynamic stiffness measurement for design of suspended handles to reduce hand-arm vibration. Basdogan and Dikmen<sup>11</sup> measured dynamic driving-point stiffness of vehicle door seal and modelled viscoelastic response with generalized Maxwell solid. A disadvantage of these methods is that a big, bulky mass is necessary for a measurement of the receptance functions. Vahdati and Saunders<sup>12</sup> described a high-frequency test machine and measured the dynamic rubber stiffness of an aircraft engine mount up to 2000 Hz. The authors indicated that with a proper design of the test fixture and the appropriate mass selection a dynamic stiffness test on the rubber mounts at frequencies as high as 5000 Hz can be performed. The downside of this method is that a conventional test machine is still needed to obtain the dynamic stiffness up to 250 Hz, and like with previous methods a big, bulky mass is needed.

This work reviews three theoretical models with a single-degree-of-freedom (SDOF) system with a ground excitation to describe the dynamic response of the rubber. Equations for an estimation of a constant Young's modulus and a constant damping factor from the transmissibility were developed. The response of the SDOF system was then measured experimentally and from it, with the developed equations, a constant damping factor and Young's modulus at the resonance frequency were evaluated for all three theoretical

models. Additionally, estimated values were used to calculate the response of theoretical SDOF systems and compared with the measurements.

Furthermore, the experimentally measured response of the SDOF system was used to identify the dynamic material properties of the rubber; the Young's modulus and the damping factor were, in this case, derived as a function of the frequency. These frequency-dependent results were then used in a finite-element analysis to predict the dynamic response of the measured system.

## Theoretical Background

A SDOF system with ground excitation that consists of an element of mass  $M$  and a linear rubber-like material, which separates the mass from a foundation that vibrates sinusoidally with an angular frequency  $\omega$ , is shown in Fig. 1. The rubber is utilized so that its behaviour is governed by the complex shear modulus  $G_\omega^*$ . Here, it is assumed that the temperature remains constant with time, so that the shear modulus may be written as<sup>13,14</sup>

$$G_\omega^* = G_\omega (1 + i\delta_{G_\omega}), \quad (1)$$

where  $G_\omega$  is the real part and  $\delta_{G_\omega}$  is the ratio of the imaginary to the real part of the complex shear modulus  $G_\omega^*$ , and is known as the damping factor and  $i$  is equal to  $\sqrt{-1}$ . Snowdon<sup>13</sup> also reported that for rubber-like materials we can write, with a negligible error, that

$$E_\omega = 3G_\omega \quad (2)$$

and

$$\delta_{E_\omega} = \delta_{G_\omega} \quad (3)$$

Similar to Eq. 1, with Eqs. 2 and 3 in mind, expression for the complex Young's modulus  $E_\omega^*$  can be written in the form

$$E_\omega^* = E_\omega (1 + i\delta_{E_\omega}), \quad (4)$$

where  $E_\omega$  is the real part and  $\delta_{E_\omega}$  is the ratio of the imaginary to the real part of the complex Young's modulus  $E_\omega^*$ , and is known as the damping factor.

Gent and Lindley<sup>15</sup> proposed a relationship between the apparent Young's modulus  $E_a$  and the Young's modulus  $E$  for bonded rubber blocks, except for those with large lateral dimensions (a large shape factor), with the expression

$$E_a = E (1 + \beta S^2) \quad (5)$$

where  $\beta$  is a numerical constant and  $S$  is a dimensionless shape factor. For samples of rubbers

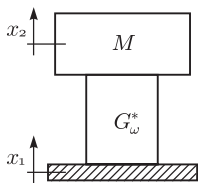


Figure 1 SDOF system with ground excitation.

that are circular, square or moderately rectangular in cross-section,  $\beta = 2^{13,15}$  and smaller values of  $\beta$  are used for carbon-black-filled vulcanizates.<sup>15</sup> The shape factor is the ratio of the area of one loaded surface to the other force-free area. The shape factor for a rubber cylinder is  $D/4h$ , where  $D$  is the diameter and  $h$  is the height of the cylinder,<sup>13</sup> and the shape factor for a cuboid is  $(d_1 d_2)/(2h(d_1 + d_2))$ , where  $d_1$  and  $d_2$  are the dimensions of the rectangular cross-section and  $h$  is the height of the cuboid.

The equation of motion for a system with a frequency-dependent Young's modulus can be written in the frequency domain as

$$-\omega^2 M x_2^* e^{-i\omega t} = (A/h) E_{a\omega}^* (x_1 - x_2^*) e^{-i\omega t}, \quad (6)$$

where  $x_1$  is the displacement of the foundation,  $x_2$  is the displacement of the mass  $M$ ,  $A$  is cross-sectional area and  $h$  height of rubber-like material, and the asterisk superscript denotes complex quantities.

From Eqs. 4 and 6 it is possible to derive the transmissibility of the system, which is defined as the magnitude of the displacement ratio

$$T = \left| \frac{x_2^*}{x_1} \right| = \frac{\sqrt{(1 + \delta_{E\omega}^2)}}{\sqrt{\left(1 - \omega^2 \frac{hM}{AE_{a\omega}}\right)^2 + \delta_{E\omega}^2}} \quad (7)$$

This is a general transmissibility equation from which the transmissibility of any linear, rubber-like material may be obtained, if the dependence of  $E_{a\omega}$  and  $\delta_{E\omega}$  on the frequency is known.

In Ref.,<sup>13</sup> certain assumptions were made about the properties of rubber-like materials that simplify the general transmissibility equation. For better referencing of the general transmissibility, Eq. 7 is written in the form

$$T = \frac{\sqrt{1 + \delta_{E\omega}^2}}{\sqrt{\left(1 - \Omega^2 \frac{E_{a0}}{E_{a\omega}}\right)^2 + \delta_{E\omega}^2}} \quad (8)$$

Here,  $\Omega = \omega/\omega_0$  is the frequency ratio,  $\omega_0^2 = (AE_{a0})/(hM)$  is the natural frequency of the SDOF system, and  $E_{a0}$  is the value of  $E_{a\omega}$  at the natural frequency.

The first simplification of Eq. 8 is called damping of the Solid Type I (sometimes referred to as hysteretic damping). This simplification is used for low-damping materials where the shear or Young's modulus and the damping vary only slowly with frequency and may be considered as constants in the frequency range of interest in vibration problems. Thus,  $E_{a0}/E_{a\omega} = 1$  and  $\delta_{E\omega} = \delta_E$ . With the use of this simplification, the transmissibility becomes

$$T_{\text{solidI}} = \frac{\sqrt{1 + \delta_E^2}}{\sqrt{(1 - \Omega^2)^2 + \delta_E^2}} \quad (9)$$

The second simplification is called damping of the Solid Type II and is used for high-damping materials, where the shear or Young's modulus increases very rapidly with frequency, and for rubbers having transition frequencies in the frequency range of interest in vibration problems. Thus, the Young's modulus is assumed to be directly proportional to the frequency and the damping factor is considered to be independent of the frequency, as in the case of damping of the Solid Type I. This can be written as  $E_{a0}/E_{a\omega} = \omega_0/\omega = 1/\Omega$  and  $\delta_{E\omega} = \delta_E$ . The expression of transmissibility, Eq. 8, becomes

$$T_{\text{solidII}} = \frac{\sqrt{1 + \delta_E^2}}{\sqrt{(1 - \Omega)^2 + \delta_E^2}} \quad (10)$$

Third simplification is called damping of the Parallel Spring and Dashpot, also known as damping of the viscous type. In this case, the rubber-like material is replaced by a spring of stiffness  $K$  and a parallel dashpot with the coefficient of viscosity  $\eta$ , as shown in Fig. 2. The transmissibility for this system is

$$T_{\text{viscous}} = \frac{\sqrt{1 + (2\Omega\delta_R)^2}}{\sqrt{(1 - \Omega^2)^2 + (2\Omega\delta_R)^2}} \quad (11)$$

where  $\Omega$  is now defined as the frequency ratio with the natural frequency, defined as

$$\omega_0^2 = \frac{K}{M} \quad (12)$$

and  $\delta_R$  is the damping ratio, defined as

$$\delta_R = \frac{\eta\omega_0}{2K} \quad (13)$$

Expressions above were derived assuming that isolator does not have any mass, but real-life isolators have some mass and as a result, wave effects may develop at high frequencies of transmitted vibrations whereas the dimensions of the isolators

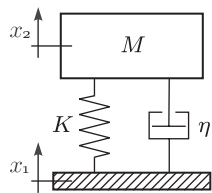


Figure 2 SDOF system mass-spring-dashpot with ground excitation.

become commensurate with multiples of the half wavelengths of the elastic waves passing through the flexible elements of the isolators as reported by Rivin<sup>16</sup> and Snowdon.<sup>13,14,17</sup> Wave frequencies are intense high-frequency peaks resulting in deterioration of transmissibility in the high-frequency range and can be seen in Fig. 6. High-frequency wave resonances in vibration isolators develop at frequencies<sup>16</sup>

$$\omega_i = i\pi \omega_0 \sqrt{\frac{M}{\rho Ah}} \quad (14)$$

where  $\omega_0$  is the fundamental natural frequency,  $i = 1, 2, 3$  is the sequential number of the resonance, and the expression under the square root is the mass ratio between the mass  $M$  of the supported object associated with the flexible element, where the total mass of the flexible element is calculated from the density  $\rho$ , the cross-sectional area  $A$  and the height  $h$ .

**Experimental Set-Up**

In the experimental set-up, a typical industrial rubber with a cross-section of 20 × 30 mm and height of 20 mm was used. The rubber was tightly glued to a cylindrical aluminium mass (83.9 g) on one end and to the specially designed head expander of a shaker on the other end, as shown in Fig. 3. In this set-up, the aluminium mass represents the rigid mass of the SDOF system in Fig. 1 and the rubber specimen provides the complex Young's modulus, which includes the damping as shown in Eq. 4. The head expander was fixed to an electromagnetic shaker (B&K type 4809) that was driven by B&K software PULSE v.13. Broadband white noise was used for the excitation signal. The transmissibility was measured with two accelerometers (B&K type 4507 B004): one was used for acquiring the input signal and the other for acquiring the output signal,  $x_1$  and  $x_2$ , respectively. The measured transmissibility function for two different rubber specimens is shown in Fig. 6.

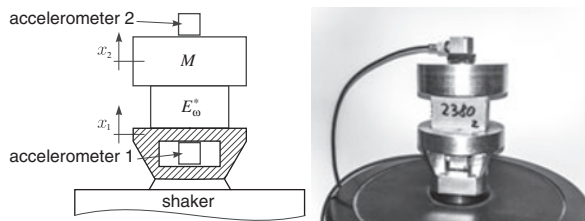


Figure 3 Experimental set-up.

**Estimation of the Young's Modulus and the Damping of the Rubber from the Measurement**

**Constant Young's modulus and damping**

Damping governs the magnitude of the transmissibility at resonance. So by using the derivative of transmissibility, Eq. 7, it is possible to determine at which frequency the maximum occurs, and with a knowledge of the maximum magnitude of the transmissibility from the measurement, the damping factor can be calculated.

From the derivative of the equation for the damping of the Solid Type I, Eq. 9, we can determine that the maximum of the transmissibility occurs at a frequency ratio  $\Omega = 1$ , which is at the natural frequency of the SDOF system. The magnitude of transmissibility at the natural frequency is

$$T_{max} = \sqrt{1 + \frac{1}{\delta_E}} \quad (15)$$

Thus by knowing the maximum of the transmissibility from the measurement, the damping factor of the Solid Type I can be calculated from Eq. 15,

$$\delta_E = \frac{1}{\sqrt{T_{max}^2 - 1}} \quad (16)$$

The same procedure can be repeated with Eq. 10 for the damping of the Solid Type II. In this case, the maximum of the transmissibility also occurs at the resonance frequency,  $\Omega = 1$ . The magnitude of the transmissibility and the damping factor at the natural frequency can be calculated from Eqs. 15 and 16. For both cases, the apparent Young's modulus at the natural frequency  $E_{a0}$  is calculated from  $\omega_0^2 = (AE_{a0}) / (hM)$  and is

$$E_{a0} = \frac{\omega_0^2 hM}{A} \quad (17)$$

where  $M$  is the total mass of the aluminium cylinder and the accelerometer 2. With respect to Eqs. 5 and 17, a constant Young's modulus is derived as

$$E_0 = E_{a0} / (1 + \beta S^2) \quad (18)$$

**Table 1** Young's modulus and damping for rubber specimen 1—rubber of hardness 40 ShA

|                | Solid Type I | Solid Type II | Parallel Spring and Dashpot |
|----------------|--------------|---------------|-----------------------------|
| $E_0$ (MPa)    | 4.297        | 4.297         | 4.315                       |
| $\delta_E$ (-) | 0.0909       | 0.0909        | —                           |
| $\delta_R$ (-) | —            | —             | 0.0455                      |

For the damping of the Parallel Spring and Dashpot, Eq. 11, the maximum of the transmissibility occurs at the frequency ratio

$$\Omega = \sqrt{\frac{\sqrt{8\delta_R^2 + 1} - 1}{4\delta_R^2}} \quad (19)$$

Referring to Eqs. 11 and 19, the maximum of the transmissibility can be calculated and then the damping ratio of the Parallel Spring and Dashpot system is given with the equation

$$\delta_R = \frac{\sqrt{2}}{2} \sqrt{\frac{T}{T^3 - T + \sqrt{\frac{1}{T^2-1}} - 2T^2 \sqrt{\frac{1}{T^2-1}} + T^4 \sqrt{\frac{1}{T^2-1}}}} \quad (20)$$

The natural frequency of the Parallel Spring and Dashpot system  $\omega_0$  is calculated from Eq. 19, and the spring stiffness  $K$  can be derived from Eq. 12. From the spring stiffness  $K$  with respect to the definition of the Young's modulus and the equation of Hook's law, it is possible to deduce apparent Young's modulus of rubber at the natural frequency

$$E_{a0} = \frac{KL_0}{A_0} \quad (21)$$

where  $A_0$  is the original cross-sectional area through which the force is applied and  $L_0$  is the original length of the object. With Eq. 18, a constant Young's modulus is calculated from apparent Young's modulus.

The estimated values of the constant Young's modulus and the damping factor, from all three theoretical SDOF systems, Eqs. 15–21, for two different rubber specimens are presented in Tables 1 and 2.

**Frequency-dependent Young's modulus and damping**

Like in Refs.<sup>3</sup> and<sup>4</sup> where the complex behaviour of the rubber was written in a different form, the frequency-dependent Young's modulus and damping factor of the rubber-like material can be calculated from the real and imaginary parts of the complex transmissibility. By writing the

**Table 2** Young's modulus and damping for rubber specimen 2—rubber of hardness 63 ShA

|                | Solid Type I | Solid Type II | Parallel Spring and Dashpot |
|----------------|--------------|---------------|-----------------------------|
| $E_0$ (MPa)    | 20.785       | 20.785        | 22.021                      |
| $\delta_E$ (-) | 0.355        | 0.355         | —                           |
| $\delta_R$ (-) | —            | —             | 0.1775                      |

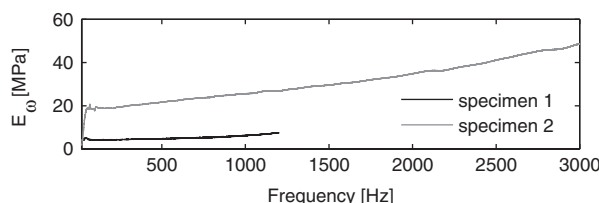


**Figure 4** Young's modulus as a function of frequency for specimen 1 (rubber of hardness 40 ShA) and specimen 2 (rubber of hardness 63 ShA).

real part  $Re(T) = Re(x_2/x_1)$  and the imaginary part  $Im(T) = Im(x_2/x_1)$ , the following relations for the frequency-dependent apparent Young's modulus and damping factor of the rubber-like material can be obtained

$$E_{a\omega} = \frac{hM\omega^2}{A} \frac{Im(T)^2 + (Re(T) - 1) Re(T)}{Im(T)^2 + (Re(T) - 1)^2} \quad (22)$$

and

$$\delta_{E\omega} = \frac{Im(T)}{Im(T)^2 + (Re(T) - 1) Re(T)} \quad (23)$$

$Re(T)$  and  $Im(T)$  can be obtained directly from the measured transmissibility, while the mass  $M$  has to be measured.

With the use of the real and imaginary parts of the measured transmissibility [ $Re(T)$  and  $Im(T)$ ], as well as Eqs. 5 and 22, it is possible to calculate the Young's modulus as a function of the frequency, as shown in Fig. 4. To estimate the frequency-dependent damping factor as a function of frequency, shown in Fig. 5, in addition to the real and imaginary parts of the measured transmissibility, Eq. 23 was also used.

**Dynamic Response Calculation**

**Calculation with theoretical SDOF systems**

Estimated constant values of the Young's modulus and the damping factors from theoretical SDOF systems, presented in Tables 1 and 2, were used to calculate the transmissibility for the damping of the Solid Type I, Eq. 9, the damping of the Solid

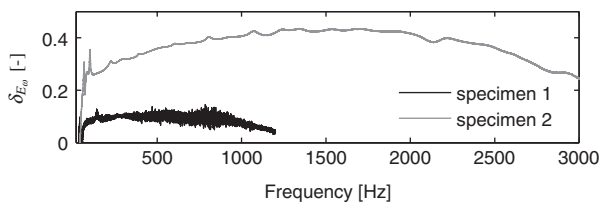


**Figure 5** Damping factor as a function of frequency for specimen 1 (rubber of hardness 40 ShA) and specimen 2 (rubber of hardness 63 ShA).

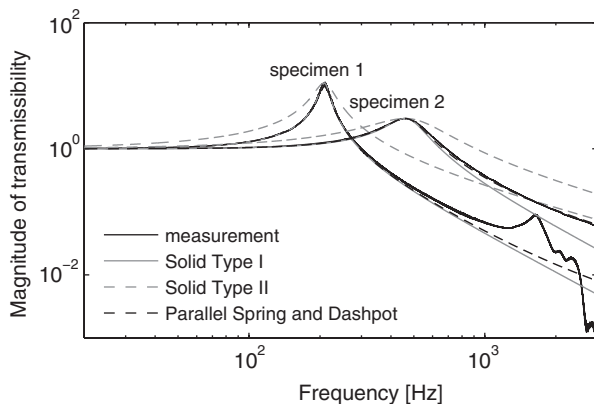


**Figure 6** Comparison of different theoretical SDOF systems with measurement for specimen 1 (rubber of hardness 40 ShA) and specimen 2 (rubber of hardness 63 ShA).

Type II, Eq. 10, and the damping of the Parallel Spring and Dashpot, Eq. 11. Figure 6 shows measured and calculated transmissibilities for two different rubber specimens (one softer 40 ShA and one harder 63 ShA).

### Finite-element analyses

Finite-element analyses were also made with ANSYS Workbench v.14 to compare the numerically calculated transmissibilities with the measured ones. The finite-element model represents a cylindrical aluminium mass with a diameter of 50 mm and a height of 15 mm, and a cuboid rubber with a cross-section of 20 × 30 mm and a height of 20 mm, and an accelerometer on the top surface of the aluminium mass, which was modelled as a mass point of 4.6 g, shown in Fig. 7. The mesh was generated with higher order 3D 20-node solid element that exhibits quadratic displacement behaviour, SOLID186 and element MASS21 for mass point. Mesh contains 5014 elements and 22,981 nodes, shown in Fig. 7. The Young's modulus of the aluminium mass was  $7.1 \times 10^{10} \text{ N/m}^2$  and the Poisson's ratio was 0.33. The density was calculated from

the measured weight of the aluminium mass (83.9 g) and was  $2848.7 \text{ kg/m}^3$ . The densities of the rubber specimens were also calculated from the masses of 14.4 g for specimen 1 and 15.1 g for specimen 2, which corresponds to densities of  $1200.0$  and  $1258.3 \text{ kg/m}^3$ , respectively. The Poisson's ratio for both rubbers was chosen near the theoretical value of 0.5 and was 0.4999. The Young's modulus and the damping factors were defined in three different ways regarding the type of analysis.

In the analysis of the transmissibility for the frequency-dependent Young's modulus and damping factor, the estimated frequency-dependent values, shown in Figs. 4 and 5, were imported into finite-element model and defined as TB,ELASTIC for the Young's modulus and TB,SDAMP for the material structural damping coefficient as frequency-dependent in commands under definition of a harmonic analysis.

In the analysis of the constant values of the Young's modulus and damping factor, the values were defined in software's Engineering Data. Special attention when defining the damping was needed for both cases. A consideration of different vibration damping using the software ANSYS is addressed in.<sup>18</sup>

In the first case with the values estimated from the theory of damping of the Solid Type I or the Solid Type II, Table 1, the damping was input as the *constant damping coefficient*  $\zeta$  where the value of damping was half of the estimated damping factor and was calculated with equation<sup>19,20</sup>

$$\zeta = \delta/2 = 0.0909/2 = 0.0455 \quad (24)$$

In the second case with the constant values from the theoretical SDOF system damping of the Parallel Spring and Dashpot, Table 1, the damping was input as the *damping factor*  $\beta$  of the Rayleigh damping, where  $\beta$  was given by ANS<sup>21</sup>

$$\beta = \frac{2\delta_i}{\omega_i}, \quad (25)$$

where  $\omega_i$  is the  $i$ th natural angular frequency and  $\delta_i$  is the damping ratio at the  $i$ th natural circular frequency. In our case  $\delta_i = \delta_R = 0.0455$  and  $\omega_i = 1311.30 \text{ rad/s}$  (208.7 Hz), which from Eq. 25 gives the stiffness matrix multiplier  $\beta = 6.9397 \times 10^{-5}$ .

The harmonic analysis for the three cases was analysed in the frequency band from 20 to 3000 Hz, with a frequency resolution of 1 Hz. The measured and calculated transmissibilities are shown in Fig. 8.

Furthermore, the numerical calculations for two different shape factors for each specimen were made,

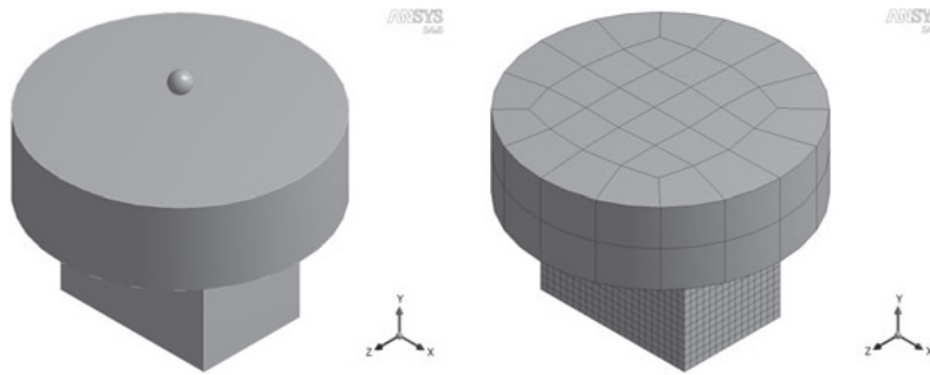


**Figure 7** Finite-element model in ANSYS Workbench v.14, model (left) and mesh (right).

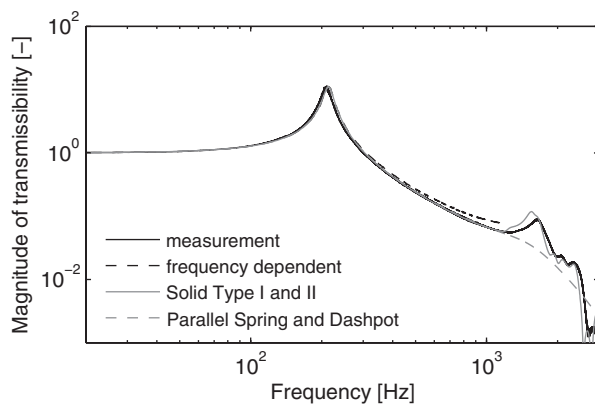


**Figure 8** Comparison of transmissibilities calculated with frequency-dependent Young's modulus and damping, constant Young's modulus and damping obtained from Solid Type I and II model and from Parallel Spring and Dashpot model with measurement for specimen 1 with a horizontal orientation (cross-section  $20 \times 30$  mm).

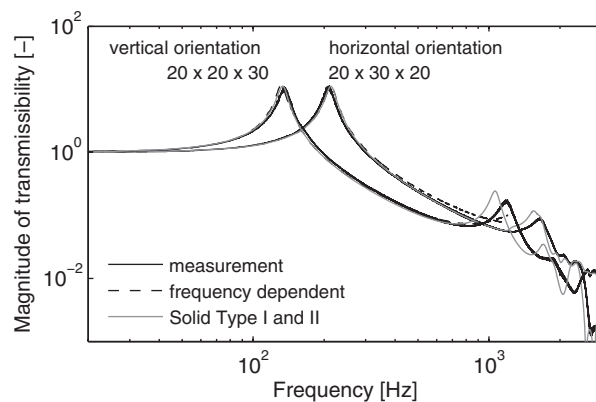


**Figure 9** Comparison of transmissibilities calculated with frequency-dependent Young's modulus and damping and constant Young's modulus and damping obtained from Solid Type I and II model with measurement for specimen 1 with a horizontal (cross-section  $20 \times 30$  mm) and vertical orientations (cross-section  $20 \times 20$  mm).

which were obtained by varying the orientation of the rubber specimen. When the rubber specimen was oriented horizontally ( $20 \times 30 \times 20$  mm<sup>3</sup>) and vertically ( $20 \times 20 \times 30$  mm<sup>3</sup>), the shape factors were 0.1667 and 0.3, respectively. The numerically calculated transmissibilities are shown in Fig. 9 for specimen 1 and in Fig. 10 for specimen 2.

## Discussion

Four rubber specimens were used in our experiments. To determine the Young's modulus and the damping two rubber specimens with a cross-section  $20 \times 30$  mm and a height of 20 mm were prepared and in the experiments the orientation of the specimens was changed to obtain four different transmissibilities.

First, the Young's modulus and the damping factor were calculated from Eqs. 15 to 21 and were

presented in Table 1 for specimen 1 and in Table 2 for specimen 2. These values were then used to calculate the transmissibilities of three simplified theoretical models named the damping of the Solid Type I, Eq. 9, the damping of the Solid Type II, Eq. 10, and the damping of the Parallel Spring and Dashpot, Eq. 11. The results can be seen in Fig. 6. We can conclude that in our case the damping of the Solid Type II was completely inappropriate for modelling the theoretical response of the rubber for both specimens. From a comparison of the results for specimen 1, it is clear that the correlation between the damping of the Solid Type I and the damping of the Parallel Spring and Dashpot with the measurement was good up to about 800 Hz, that is, approximately four times the natural frequency, and from here on both of the theoretically calculated transmissibilities start to deviate significantly from the measurement. Also, from

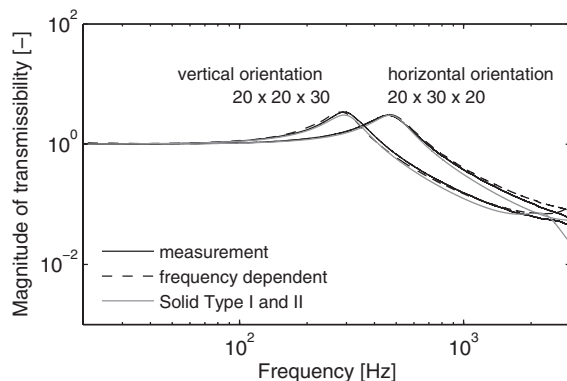


**Figure 10** Comparison of transmissibilities calculated with frequency-dependent Young's modulus and damping and constant Young's modulus and damping obtained from Solid Type I and II model with measurement for specimen 2 with a horizontal (cross-section  $20 \times 30$  mm) and vertical orientations (cross-section  $20 \times 20$  mm).

a comparison of the results of specimen 2 it is clear that the damping of the Solid Type I does not agree well with the measurement in the higher frequency range, since the damping value was higher, but not high enough to obtain good approximation of the response with the damping of the Solid Type II; however the Parallel Spring and Dashpot model shows better agreement in the considered frequency range.

At higher frequencies, the deterioration of the measured transmissibility can be seen and is a consequence of wave effects. While the natural frequency of specimen 1 is 208.7 Hz, the first theoretical wave frequency, Eq. 14, is 1626.77 Hz, which is in good agreement with the measurement, where an intense peak resulting in a deterioration of the transmissibility can be seen at 1644 Hz.

Second, the frequency-dependent Young's modulus and damping factor were calculated where the real and imaginary parts of the measured transmissibility and Eqs. 5, 22, and 23 were used. The frequency-dependent values are presented in Figs. 4 and 5. The conclusion can be drawn that the Young's modulus and the damping factor of specimen 1 may be used only in the frequency range up to 1200 Hz, while in the higher frequency range the calculations were not correct due to the wave effects, which the SDOF system does not take into account, as well as the measurement noise. The estimated values of the Young's modulus and the damping factor in the case of specimen 2 seem to be in good agreement with our expectations for the considered frequency range.

From this the general conclusion can be made that the frequency range for which the frequency-dependent values can be calculated mostly depends

on the Young's modulus and the dimensions of the rubber. The dimensions and the Young's modulus govern the natural frequency of the SDOF system with the integrated rubber, and the higher the natural frequency is, the higher in the frequency range the values of the dynamic material properties can be calculated.

Several finite-element analyses were carried out to verify the use of the estimated values of the Young's modulus and the damping factor in the finite-element model.

Three types of modelling with respect to damping in ANSYS Workbench v.14 were presented in Fig. 8, where good agreement of the finite-element analysis with the frequency-dependent values and the constant values obtained from the SDOF system with damping of the Solid Type are shown, but the numerically calculated transmissibility where the damping was input as the damping factor  $\beta$  starts to deviate significantly from the measurements at higher frequencies. The calculated values of the damping factor for specimen 1, Fig. 5, were useful only up to 1200 Hz; therefore, the transmissibility was only calculated up to this frequency. Consequently, it was not possible to make any conclusions about the transmissibility in the frequency range above 1200 Hz. It should also be noted that the numerically calculated transmissibility, where the damping was defined as a *constant damping coefficient*, shows good agreement with the measurement also in the high-frequency range where the internal natural frequencies of the rubber occur.

A further four types of finite-element analyses were made (two on each specimen), where two different orientations of rubber were analysed (horizontal and vertical). All the values were estimated for a horizontal orientation of the rubber specimens and applied to a finite-element analysis of the rubber specimen in a horizontal and vertical orientations and compared with the measurements. For the analyses with specimen 1, Fig. 9, similar conclusions could be made as for the previous analysis in Fig. 8. Finite-element analyses with the rubber specimen 2, Fig. 10, showed that the transmissibilities calculated with frequency-dependent values showed better agreement with the measurements than the transmissibilities calculated with constant values, but the transmissibilities for all cases were in good agreement with the measurements.

On the basis of the presented finite-element analyses, it can be concluded that the Young's modulus and the damping factor of rubbers with a small variation of the dynamic material properties,



like specimen 1 in our case, could be modelled as constants, where the damping has to be input as a *constant damping coefficient* not as  $\beta$  in the Rayleigh damping.

To obtain the Young's modulus and the damping factor for the considered rubber up to the higher frequency range, the natural frequency of the SDOF system has to be high, meaning the dimensions of the rubber have to be chosen accordingly. The use of reduced-variables method,<sup>2</sup> where experimental curves gained at different temperatures are gathered into a unique curve called the master curve for the Young's modulus is also an option.

A potential source of error is the 0.1 mm variation in the dimensions of the rubber, which is a result of cutting the rubber to the desired dimensions. This effect introduces some uncertainty in calculating the shape factor  $S$ , on which the Young modulus depends a great deal. A second potential source of error is the lack of knowledge about the exact value of the Poisson's ratio of the rubber for the input parameter in ANSYS. Theoretically, the Poisson's ratio of the rubber is 0.5, but as rubbers may contain other additives the Poisson's ratio is rarely equal to 0.5, but is usually somewhat smaller. Sim and Kim<sup>3</sup> reported that for rubbers with large shape factors the Poisson's ratio has a great influence on the Young's modulus. In the literature, the effective compression modulus was derived<sup>22–25</sup> instead of the apparent Young's modulus and its dependence on the Poisson's ratio and the shape factor was shown. Optimization process calculating natural frequencies of plates in finite-element model solver were also made, where values of the Young's modulus and the Poisson's ratio were varied and natural frequencies were compared with measured values,<sup>26</sup> but with this method only constant values of Young's modulus and Poisson's ratio for natural frequency could be determined.

## Conclusions

The technique presented in this paper provides a relatively quick and easy way to evaluate the frequency-dependent Young's modulus and damping factor of rubber-like materials.

Three types of modelling for the dynamic material properties of rubber-like materials in finite-element analyses were presented. The results show that the shear modulus and consequently the Young's modulus for these two studied materials change only slightly with frequency and could eventually, in finite-element analyses, also be modelled as constants.

Two sources of potential errors were identified. The first was due to the variation in the dimensions of the rubber specimens and the second due to a lack of knowledge about the Poisson's ratio of the rubber.

## Acknowledgments

The Operation part was financed by the European Union, European Social Fund.

## References

1. Nashif, A.D., Jones, D.I.G., and Henderson, J.P., *Vibration Damping*, John Wiley and Sons, New York (1985).
2. Ferry, J.D., *Viscoelastic Property of Polymers*, Wiley, New York (1970).
3. Sim, S., and Kim, K.J., "A Method to Determine the Complex Modulus and Poisson's Ratio of Viscoelastic Materials from Fem Applications," *Journal of Sound and Vibration* **141**(1): 71–82 (1990).
4. Ramorino, G., Vetturi, D., Cambiaghi, D., Pegorett, A., and Ricco, T., "Developments in Dynamic Testing of Rubber Compounds: Assessment of Non-Linear Effects," *Polymer Testing* **22**: 681–687 (2003).
5. Caracciolo, R., and Giovagnoni, M., "Frequency Dependence of Poisson's Ratio using the Method of Reduced Variables," *Mechanics of Materials* **24**: 75–85 (1996).
6. Caracciolo, R., Gasparetto, A., and Giovagnoni, M., "Application of Causality Check and of the Reduced Variable Method for Experimental Determination of Young's Modulus of a Viscoelastic Material," *Mechanics of Materials* **33**: 693–703 (2001).
7. Lin, T.R., Farag, N.H., and Pan, J., "Evaluation of Frequency Dependent Rubber Mount Stiffness and Damping by Impact Test," *Applied Acoustics* **66**: 829–844 (2005).
8. Ooi, L.E., and Ripin, Z.M., "Dynamic Stiffness and Loss Factor Measurement of Engine Rubber Mount by Impact Test," *Materials and Design* **32**: 1880–1887 (2011).
9. Nadeau, S., and Champoux, Y., "Application of the Direct Complex Stiffness to Engine Mounts," *Experimental Techniques* **24**(3): 21–23 (2000).
10. Hao, K.Y., Ean, O.L., and Ripin, Z.M., "The Design and Development of Suspended Handles for Reducing Hand-Arm Vibration in Petrol Driven Grass Trimmer," *International Journal of Industrial Ergonomics* **41**: 459–470 (2011).
11. Basdogan, I., and Dikmen, E., "Modeling Viscoelastic Response of Vehicle Door Seal," *Experimental Techniques* **35**(3): 29–35 (2011).
12. Vahdati, N., and Saunders, L.K.L., "High Frequency Testing of Rubber Mounts," *ISA Transactions* **41**: 145–154 (2002).

13. Snowdon, J.C., *Vibration and Shock in Damped Mechanical Systems*, John Wiley and Sons, New York (1968).
14. Snowdon, J.C., "Vibration Isolation: Use and Characterization," *Journal of the Acoustical Society of America* **66**(5): 1245–1274 (1979).
15. Gent, A.N., and Lindley, P.B., "The Compression of Bonded Rubber Blocks," *Proceedings of the Institution of Mechanical Engineers* **173**: 111–122 (1959).
16. Rivin, E., "Vibration Isolation Theory," Braun, S., (ed), *Encyclopedia of Vibration*, Academic Press, London, UK, pp. 1487–1506 (2002).
17. Snowdon, J.C., "The Cohice of Resilient Materials for Anti-Vibration Mountings," *British Journal of Applied Physics* **9**(12): 461–469 (1958).
18. Cai, C., Zheng, H., Khan M.S., and Hung, K.C. "Modeling of material damping properties in ansys," URL <http://www.ansys.com/Resource+Library/Conference+Papers/Modeling+of+Material+Damping+Properties+in+ANSYS> (2011).
19. ANS. ANSYS Workbench Help: //Command Reference//XXI. T Commands//TB. ANSYS, Canonsburg, PA (2012a).
20. ANS. ANSYS Mechanical Linear and Nonlinear Dynamics, Customer training material. ANSYS, Canonsburg, PA (2011).
21. ANS. ANSYS Workbench Help: //Structural Analysis Guide//1. Overview of Structural Analyses//1.4. Damping. ANSYS, Canonsburg, PA (2012b).
22. Tsai, H.C., and Lee, C.C., "Compressive Stiffness of Elastic Layers Bonded Between Rigid Plates," *International Journal of Solids and Structures* **35**(23): 3053–3069 (1998).
23. Koh, C.G., and Lim, H.L., "Analytical Solution for Compression Stiffness of Bonded Rectangular Layers," *International Journal of Solids and Structures* **38**: 445–455 (2001).
24. Tsai, H.C., "Compression Analysis of Rectangular Elastic Layers Bonded Between Rigid Plates," *International Journal of Solids and Structures* **42**: 3395–3410 (2005).
25. Pinarbasi, S., Akyuz, U., and Mengi, Y.. "Uniform Compression of Bonded Elastic Layers," *Fourth International Conference on Earthquake Engineering*, Taipei, Taiwan; 2006.
26. Pagnotta, L., and Stigliano, G., "Assessment of Elastic Properties of Isotropic Plates by Dynamic Tests," *Experimental Techniques* **34**(2): 19–24 (2010).